UNIVERSITY OF CALIFORNIA, SAN DIEGO

Restricted Spectrum Imaging Demonstrates Decreased Neurite Density in Patients with Mesial Temporal Lobe Epilepsy

A thesis submitted in partial satisfaction of the requirements for the degree

Master of Science

in

Biology

by

Richard Qi Zhi Loi

Committee in charge:

Professor Carrie McDonald, Chair
Professor Brenda Bloodgood, Co-Chair
Professor Jill Leutgeb

2016

The Thesis of Richard Qi Zhi Loi is approved, and is acceptable in quality and form for publication on microfilm and electronically:

_____

_____

Co-Chair

_____

Chair

University of California, San Diego

2016

DEDICATION

I dedicate this thesis to my family, Bach, Amy, and Vivian for the unconditional love and support they have given me.

TABLE OF CONTENTS

LIST OF FIGURES

LIST OF TABLES

ACKNOWLEDGEMENTS

I would first like to thank Professor Carrie McDonald for the many years that she has mentored and guided me as a member of her laboratory. Those of us who work with Carrie know the magnitude of the burden she bears and the intelligence she possesses to navigate towards her goals. Always willing to carve out time for her team, her model of kindness in accomplishment will undoubtedly guide my own work in the future. I am forever grateful for her guidance.

I would like to also thank Kelly Leyden, our former research associate and fellow lab team member, for teaching me data structure and navigation in my early years as an assistant. Her contributions in data acquisition, guidance and friendship were cherished by all of our team.

I would also like to thank Professor Brenda Bloodgood and Professor Jill Leutgeb for being members of my committee.

Next, I would like to thank my research assistant Akshara Balachandra for his support coding the many scripts that made this computationally intensive project possible. In addition, I would like to thank Holly Hasler for her work in data acquisition, Nobuko Kemmotsu and Erkut Kucukboyaci for their guidance in my first year as an assistant.

Lastly, I would like to thank all my friends who have been with me every step of this journey through undergraduate years and this graduate degree.

ABSTRACT OF THE THESIS

Restricted Spectrum Imaging Demonstrates Decreased Neurite Density in Patients with Mesial Temporal Lobe Epilepsy

by

Richard Qi Zhi Loi

Master of Science in Biology

University of California, San Diego, 2016

Professor Carrie McDonald, Chair

Professor Brenda Bloodgood, Co-Chair

Temporal lobe epilepsy (TLE) is a debilitating neurological condition that is physiologically characterized by pathological changes to the hippocampus and proximal tissues. Diffusion tensor imaging (DTI) has repeatedly shown that patients with TLE also have microstructural changes to temporal and extratemporal white matter unseen in traditional structural imaging. Previous DTI studies have shown decreased fractional anisotropy (FA), a measure representing directionality of diffusion, in patients with TLE compared to controls. The systematic decline of FA observed along major white matter tracts in TLE is often interpreted as a loss of integrity of white matter. However, FA is a

nonspecific measure that is heavily influenced by not only axonal loss, but also by extracellular changes (i.e., edema, inflammation) and crossing fibers.

In 21 patients with TLE and 11 age-matched controls, we aim to better characterize underlying white matter changes in TLE using a new diffusion model, Restricted Spectrum Imaging (RSI) that separates intracellular changes in diffusion (i.e., neurite density; ND) from extracellular changes (isotropic free water; IF) and crossing fibers (CF). Using both voxelwise and tract-based analysis, we demonstrate that both FA and ND measures have a high level of spatial correspondence, meaning the loss of directionality is primarily driven by the loss of diffusion derived from restricted neurite components, rather than increases in free water or the effects of CF. In addition, changes in ND, but not FA, were associated with disease duration, suggesting that ND may provide a more specific marker of white matter disease burden in refractory TLE.

INTRODUCTION

1.1 Epilepsy

Epilepsy is a neurological condition characterized by abnormally firing neurons within grey matter. Epidemiologically, this disorder affects between 1.6% and 5.1% of all people worldwide (Banerjee et al., 2009). Of the affected individuals, approximately 26% are pharmaceutically resistant to anti-epileptic drugs (AEDs) (Berg et al., 2009). Temporal lobe epilepsy (TLE) is diagnosed by seizures that are electrographically localized to the temporal lobe (Gastaut et al., 2007). TLE is the most commonly localized seizure type and is highly pharmaceutically resistant (Engel et al., 2003). The prevention of recurrent seizures is critical for reducing cognitive and psychiatric comorbidities of epilepsy, as well as sudden death (Tellez-Zenteno, 2007).

Mesial temporal lobe sclerosis (MTS) is the most common histopathological abnormality in TLE and is characterized by a lesion of the hippocampus, amygdala and/or entorhinal cortex generally ipsilateral to the side of seizures. MTS is characterized by patterns of neuronal loss and gliosis (Wieser et al., 2004). It is currently inconclusive as to whether MTS is the cause or consequence of seizures in histologically abnormal patients (Wong et al., 2013). The identification of MTS however, greatly improves the chances of seizure freedom post-surgery (Engel et al., 2003). Imaging techniques used to identify lesions like MTS have relied on standard structural imaging protocols, such as T1-weighed imaging to visually identify hippocampal asymmetry or T2-weighted hyper intensities. However, in addition to MTS, there is considerable white matter pathology in

many patients with TLE and these white matter abnormalities are rarely seen on standard clinical imaging. Thus, more advanced forms of imaging are needed to detect occult white matter pathology in TLE.

1.2 DTI in Epilepsy

Diffusion Magnetic Resonance Imaging (dMRI) has, since the 1980s, served as a critical tool for understanding underlying brain structure and organization not apparent with traditional structural MRI. An extension of dMRI, diffusion tensor imaging (DTI), has been utilized for hundreds of studies of the brain involving many pathologies. DTI tractography measures the macroscopic interconnections between different brain regions, known as white matter tracts, by detecting overall anisotropic movement of water along these white matter tracts (Assaf et al., 2008). Water molecules diffuse most readily along the primary direction of axon bundles as opposed to perpendicular to them. DTI utilizes measurements of both perpendicular and parallel movement, in multiple gradient directions to extract the overall diffusivity parallel and perpendicular to the bundles (Pierpaoli et al., 1996). These data yield a tensor, from which different diffusion measurements are extracted, with the most popular being fractional anisotropy (FA) and mean diffusivity (MD). The former is a scalar value between zero and one describing the degree of anisotropy of diffusion along the primary fiber orientation. The latter is a scalar value between zero and one describing the total degree of isotropic diffusion within a defined space, usually a region of interest, tract or unit of three dimentional space

(voxel). Reductions in FA and increases in MD are believed to represent axonal loss and atypical myelin in patients with different neurological diseases.

One of the primay objectives of neuroimaging in epilepsy is to identify and localize abnormal tissues responsible for epileptogenic activity as an additional datapoint so that better sugical decision making and outcomes can be established. With as drastic as temporal lobe resections are, the success rate of such a proceedure in achieving long term seizure freedom is 66% (Téllez-Zenteno et al., 2005). As cognitive outcomes of surgeries are weighed against the benefits of seizure freedom in deciding for or against proceeding with a surgury, another measure potentially more sensitive to epileptogenic tissue could serve as an additional data point in confirming lateralization and localization prior to the decision to undergo surgery. There is thus a need for targeted research into the diffusion properties of particular regions of white matter proximal to epileptogenic tissue for the sake of better understanding the benefits and consequences of planned resections.

Previous DTI studies in TLE have shown widespread white matter abnormalities in patients with TLE in comparison to controls (Vulliemoz et al., 2011). Large scale studies of diffusion with traditional DTI diffusion protocols have shown wide spread abnormalities, but with pitfalls (Assaf et al., 2008). Evidence in these TLE studies, as outlined in a recent review, has shown tracts proximal to the temporal lobe such as the uncinate fasciculus (UNC), cingulum bundle (CING), inferior longitudinal fasciculus (ILF), external capsule, and arcuate fasciculus to be most affected, with distal tracts found to be affected to a lesser degree (Otte et al. 2012). Of note is the fact that the fornix (FX) in a recent meta-analysis was found to be not significant in spite of its role as one of

the primary connections to and from the hippocampus. As noted by Otte et al., most studies looked at in the meta-analysis did not use any correction for partial volume averaging, likely leading to artifacts from neighboring cerebral spinal fluid (CSF) and furthermore potentially obscuring group differences. For this study, a subsection of the FX that is resistant to partial voluming was utilized as a substitute measure of the FX as a whole.

1.3 DTI Vulnerabilities

DTI is a problematic diffusion model primarily because of the assumptions made in its creation and usage. Measures derived from this model, such as FA, MD, and others characterize the diffusion profile of averaged diffusion distances in three-dimensional space. The diffusion profile is thus unable to elaborate as to whether the profile is driven primarily due to restricted (small diffusion distance; i.e., intracellular) or free (large diffusion distance; i.e., extracellular) diffusion changes. This limitation is due to the DTI assumption of a perfect Gaussian distribution of diffusion directions for water molecules (Basser et al. 2002). The diffusion properties of water in a biological system are non-Gaussian, and are thus improperly modeled with the monoexponential function driven by the single diffusion weighing gradient and encoding properties (b-value) as called for by most standard DTI acquisition protocols (Niendorf et al., 1996). In addition to the deficient number of b-values, the direction by which the diffusion gradient is generated in DTI has been in flux, with earlier empirically derived values ranging from about twenty to the minimal six and finally thirty in the last decade (Correia et al., 2009). These

limitations of DTI result in the inability to model different diffusion compartments within a voxel, as well as to model complex fiber orientation (i.e., crossing fibers).

For DTI in epilepsy, challenges remain that are not so easily answered with a single b-value and low diffusion directions. DTI analysis in epilepsy is limited to white matter due to sampling limits. Units of three dimensional space, or voxels, in many studies are samples of 2.5mm cubes. This space sampling limits the accuracy of derived diffusion values from cortex with an average thickness of 1.5 to 4.5mm (Carpenter et al, 1995). This problem is often referred to as partial voluming, given the probability of sampling heterogeneous space at grey/CSF and grey/white boundaries. In probing at a restricted scale of diffusion, one aim is to better suppress confounding signals from these borders. White matter is a more interesting target of investigation from an architectural standpoint, as it can be better simplified by its anisotropy, or directionality, of diffusion within the tissue. This diffusion is theoretically an indirect measure of the organization of bundles of axons and their myelin sheaths (Beaulieu, 2001). This noninvasive measure of diffusion is a surrogate measure for pathology in studies of diffusion in epilepsy, with disrupted white matter pathways connecting distant regions of the brain as a point of focus. By removing confounding factors, such as loss of anisotropic signal in regions of crossing fibers, a more robust understanding of diffusion in pathological conditions like epilepsy can be realized. For a detailed review of the many pitfalls affecting DTI, readers are suggested to read a summary by the Cerignani laboratory (Jones et al., 2010)

Many patients with TLE who have sclerotic damage and volume loss to the hippocampus ipsilateral to the seizure onset are affected. There is inconclusive

knowledge about how this damage, due to initial pathology or from seizures, affects white matter tracts throughout the brain. (Gross et al., 2011) There is much still to learn about efferent and afferent white matter pathways that anatomically connect to the hippocampus in terms of seizure pathology. However, in order to better elucidate the nature of white matter damage within these pathways, more sophiticated diffusion models are greatly needed. The purpose of this study is to examine the underlying white matter pathology in TLE patients utilizing an advanced, quantitative MRI method that overcomes many of the limitations of traditional DTI models.

1.4 Advance Diffusion Protocols

In recent years, a number of advanced diffusion methods have emerged that extend beyond the tensor model and may provide more sensitive and/or specific measures of cerebral pathology in TLE. These advanced methods generally expand on DTI by the inclusion or combination of additional multiple diffusion weighing gradients, additional diffusion directions and fiber modeling. Additional b-values serve to better plot non-Gaussian diffusion signal decay, thereby better probing small scale diffusion on the order of potentially intracellular diffusion. Greater numbers of encoded diffusion directions in MRI protocols allow for better estimation of fiber orientations, especially in regions with two or more crossing fibers. Finally, fiber bundle modeling better quantifies fiber diffusion properties through a computational approach to better understand the properties of the derived diffusion signal.

Diffusion kurtosis imaging (DKI), which probes non-Gaussian diffusion and

estimates diffusion heterogeneity by expanding b-value utilization, has been applied in several studies of children and adults with TLE (Jensen et al., 2005). These studies have suggested that kurtosis measures reveal a broader and more robust pattern of microstructural abnormalities in TLE compared to conventional DTI, which may reflect DKI's greater sensitivity to multiple pathologic factors including cell loss, inflammation, and axonal and dendritic reorganization. In addition, *diffusion spectrum imaging* (DSI), a high-angular diffusion imaging (HARDI) technique, has recently been combined with a multi-compartment diffusion model, the *neurite orientation dispersion and density imaging* (NODDI) model, to estimate structural connectivity and network properties in TLE (Lemkaddem et al., 2014). This study revealed that reduced FA in the medial temporal lobes was primarily driven by reductions in intracellular diffusion, commensurate with *neurite* loss (i.e., cell and axonal loss), whereas reduced FA in extratemporal regions was also driven by fiber orientation changes, potentially reflecting disorganized fiber orientation and packing. These studies suggest that advanced diffusion techniques, which aim to resolve intravoxel tissue properties, may provide more sensitive measures of network pathology in TLE.

In this study, we apply a new multi-compartment diffusion model, *restriction spectrum imaging (RSI),* which combines key properties of these existing methods to resolve whether decreases in FA in patients with TLE are better explained by decreased axonal/neurite density (ND), crossing fibers (CF), and/or increases in extracellular diffusion (i.e., isotropic free water; IF) (White et al., 2013). This new method is an extension of traditional HARDI techniques for reconstructing crossing fibers and modeling complex orientation and structure, but with a clinically-feasible scan time (4-7

min). Using multiple diffusion weightings (*b*-values), RSI further distinguishes hindered and restricted diffusion pools in the extracellular and intracellular compartments, respectively, and models both spherically-restricted (within cells) and cylindrically restricted (within axons) diffusion. Isolating the anisotropic, restricted compartment within axons is important as this allows for estimates of the axonal density and orientation distribution that are distinct from changes in extracellular diffusion. Thus, RSI's ability to probe both the scale and geometry of tissue microstructure positions it well to determine whether regional reductions in DTI-derived FA values are due to axonal loss/demyelination versus extracellular changes (e.g., inflammation) or crossing fibers.

MATERIALS AND METHODS

2.1 Participants

This study was approved by the Institutional Review Board at the University of California, San Diego (UCSD) and all participants provided informed consent according to the Declaration of Helsinki. Twenty-one patients with medically refractory TLE and 11 age-matched controls had volumetric MRI, DTI/RSI, and clinical data that allowed for inclusion in the study. All patients were under evaluation for surgical treatment at the UCSD Epilepsy Center. They were diagnosed with medically refractory epilepsy by board-certified neurologists with expertise in epileptology, according to the criteria defined by the International League Against Epilepsy. Patients were classified into left TLE (LTLE; n=10) or right TLE (RTLE; n=11) based on seizure onsets recorded by video-EEG, seizure semiology, and neuroimaging results. Where clinically indicated, patients underwent Phase II video-EEG monitoring using 5-contact foramen ovale electrodes to exclude bilateral independent seizure onsets. Clinical MRI scans were available on all patients (i.e., T1-weighted, T2-weighted, and coronal FLAIR sequences with 1mm slices through the MTL). MRIs were visually inspected by a board-certified neuroradiologist for detection of mesial temporal sclerosis (MTS) and the exclusion of contralateral temporal lobe structural abnormalities. In 8 patients, MRI findings suggested the presence of ipsilateral MTS. No patients showed evidence of contralateral MTS or extra-hippocampal pathology on clinical MRI. Control participants were screened for neurological or psychiatric conditions.

2.2 MRI acquisition

All patients were seizure-free per self-report for a minimum of 24 hours prior to the MRI scan (Sabsevitz et al., 2003). All the brain imaging was performed on a General Electric Discovery MR750 3T scanner with an 8-channel phased-array head coil. Image acquisition included a conventional three-plane localizer, GE calibration scan, a T1-weighted 3D structural scan (TR = 8.08 msec, TE = 3.16 msec, TI = 600 msec, flip angle = 8°, FOV = 256 mm, matrix = 256 x 192, slice thickness = 1.2mm), and for standard diffusion MRI, a single-shot pulsed-field gradient spin-echo EPI sequence (TE/TR = 96ms/17s; FOV = 24cm, matrix = 128x128x48; axial). Diffusion data used for the standard DTI analysis were acquired with b-value = 0 and 1000 mm^2/s with 30 unique gradient directions. Diffusion data used for the RSI analyses were acquired with b = 0, 500, 1500, and 4000 s/mm^2, with 1, 6, 6, and 15 unique gradient directions for each b-value, respectively (total RSI scan time = ~7min). For use in nonlinear B0 distortion correction, two additional b=0 volumes were acquired with either forward or reverse phase-encode polarity.

2.3 Diffusion image processing

Preprocessing of the diffusion data included correction for B_0 distortion, eddy current distortions, gradient nonlinearity distortions, and head motion, as well as registration to the T_1-weighted structural image. For B_0 distortion correction, a reverse gradient method was used. This method provides superior accuracy and better cross-modality registration relative to the field mapping approach.

DTI-derived FA and MD were calculated based on a tensor fit to the $b = 1000$ data. Conversely, RSI utilizes a multi-b-shell acquisition in conjunction with a linear mixture model to isolate diffusion signals from separable hindered, restricted, and free water diffusion compartments within a voxel. Technical details describing the RSI mathematical framework are described in full elsewhere. RSI-based measures of ND, CF, and IF were calculated from the estimated volume fraction of the cylindrically-restricted compartment (ND), the 4^{th} order spherical harmonic component of the cylindrically-restricted compartment (CF), and the isotropic free water compartment (IF), respectively. The RSI model was fit to the data using least-squares estimation with Tikhonov regularization.

2.4 Whole Brain Map Processing

Individual T1-weighted images were iteratively registered to form a group-wise map using the Advanced Normalization Tools-Symmetric Normalization (ANTS-SyN) ver-1.9.4 algorithm (Avants et al. 2011). A group-wise T1-weighted template was formed for both LTLE and RTLE cohorts through the ANTS toolbox (Klein et al. 2010). Individual T1 warps to the group-wise template were applied to individual whole-brain FA, MD, ND, CF, and IF maps to better register maps by avoiding logical circularity in intra-measure registrations (Tustison et al. 2014). Measure maps were smoothed with a 2.5mm full-width at half-maximum Gaussian kernel. The measure maps where further binarized with white matter selections generated by FMRIB's Automated Segmentation Tool (FAST) at default settings using individual registered T1-weighted images (Zhang

et al. 2001). Statistical comparisons were performed with a general linear model design of a two independent sample t-test with 5000 iterations run on FSL Randomize that identified voxel-wise measure differences between RTLE, LTLE, and healthy controls (Winkler et al., 2014). The Threshold-Free Cluster Enhancement (TFCE) method was utilized with three dimensional voxel optimization, –T1 parameters, to enhance clustering (Smith et al. 2009).

2.6 Fiber Tract Calculations

Fiber tract FA, MD, ND, CF, and IF values were derived using a probabilistic diffusion tensor atlas that was developed using in-house software written in Matlab and C++ (i.e., AtlasTrack). A full description of the atlas and the steps used to create the atlas are described elsewhere (Hagler et al., 2009). For each participant, T1-weighted images were used to nonlinearly register the brain to a common space, and diffusion tensor orientation estimates were compared to the atlas to obtain a map of the relative probability that a voxel belongs to a particular fiber given the location and similarity of diffusion orientations. Voxels identified with FreeSurfer's automated brain segmentation as cerebrospinal fluid or gray matter were excluded from the fiber ROIs (Fischl et al., 2002). Average diffusion metrics (i.e., FA, MD, ND, CF, and IF) were calculated for each fiber ROI, weighted by fiber probability, so that voxels with low probability of belonging to a given fiber contributed minimally to average values. In the current study, this probabilistic atlas-based method was used to reconstruct the following right and left hemisphere fiber tracts due to evidence of their disruption in TLE (Diehl et al., 2008):

FX, CING, UNC, ILF, parahippocampal cingulum (PHC), and the inferior frontal occipital fasciculus (IFOF) (see Figure 1).

2.7 Statistical Analysis

Analysis of variance (ANOVAs) and independent t-tests were used to test for differences among the groups in key demographic and clinical variables. Whole-brain voxel-based analysis (VBA), comparing patients with LTLE and RTLE to controls, was performed for DTI (FA and MD) and RSI (ND, CF, and IF) metrics using voxelwise t-tests. Tract-based region of interest (ROI) analyses were also performed between each patient group's ipsilateral and contralateral fiber tracts and those of controls for each fiber tract using t-tests. Pearson correlations were used to examine relationships between our diffusion measures and clinical variables (i.e., age of seizure onset, disease duration, and seizure frequency). For both the VBA and fiber ROI analysis, $p<.005$ was used to correct for multiple comparisons.

RESULTS

3.1 Patients

Table 1 displays demographic and clinical variables for the patient and control groups. There were no statistically significant differences among the controls, LTLEs, or RTLEs in age, (F [2,29] = .634, $p > .05$). However, there was a group difference in years of education (F [2,29] = 4.02, $p<.05$) with controls achieving a higher level of education than either patient group. The distribution of gender across the three groups was comparable (*Fisher's exact test*; $\chi^2[2] = 1.90$, $p > .05$). There were no statistically significant differences between the two patient groups in disease duration ($t[17] = 1.63$, $p > .05$), age at seizure onset (t [17]= -.77, $p > .05$), seizure frequency ($t[17] = .47$, $p > .05$), or the number of patients with MTS ($\chi^2[1] = 1.56$, $p > .05$). However, the volume of the ipsilateral hippocampus was slightly smaller in patients with LTLE compared to those with RTLE ($t[19] = -2.44$, $p = .025$). Contralateral hippocampal volumes did not differ between the patient groups ($t[19] = .51$, $p > .05$). Both patient groups' ipsilateral hippocampal volumes were smaller when compared to the corresponding side of the controls volumes ($t[19] = 4.09$, $p = .001$, and $t[20] = 2.50$, $p = .04$, LTLE and RTLE, respectively), but their contralateral hippocampal volumes were not statistically different from the controls ($t[19] = .508$, $p > .05$, and $t[20] = .93$, $p > .05$, LTLE and RTLE, respectively).

3.2 VBA Analysis

Figure 2 displays voxelwise maps of significant decreases in FA, MD, ND and increases in IF in each patient group compared to controls. As can be seen, patients with LTLE showed decreased FA primarily in the left anterior temporal lobe with smaller regions of decreased FA in the inferior prefrontal and retrosplenial white matter. Compared to FA, ND maps revealed a broader and more robust pattern of decreases in LTLE, but with strong lateralization to the left hemisphere. In addition, small areas of increased IF are observed in left temporal lobe regions in and around regions of decreased ND.

In patients with RTLE, there were no regions in which decreased FA survived our $p<.005$ threshold in the voxelwise analysis. However, a more lenient threshold ($p<.02$) showed a similar pattern of decreased FA as that observed in LTLE. Similar to the pattern seen in LTLE, ND maps in RTLE revealed a broad and robust pattern of ND decreases, but with strong lateralization to the right temporal lobe region. Minimal increases in IF were noted. There were no suprathreshold differences in CF between controls and patients with LTLE or RTLE in the voxelwise analysis.

3.3 Tract-based analysis

Because patients with LTLE and RTLE showed a similar pattern of reductions in FA and ND that differed mostly in magnitude (i.e., LTLE showed more pronounced reduction in FA relative to RTLE), we combined the patient groups to examine diffusion parameters in ipsilateral and contralateral fiber tracts (see Table 2). Patients with TLE showed ipsilateral and contralateral reductions in FA and ND in the FX, CING, PHC,

UNC and ILF. In addition, ND only was reduced in the ipsilateral IFOF. Complementing our voxelwise analysis, the magnitude of the effects was consistently larger with ND than with FA (Cohen's *d*) particularly in the contralateral UNC and ipsilateral IFOF where effect sizes for ND were 33 and 66% higher, respectively. In addition, increases in IF and MD were observed in the ipsilateral FX [$t(30) = -3.5$, $p = .001$) for IF; $t(30) = -3.0$, $p = .004$ for MD] and PHC [$t(30) = -3.3$, $p = .002$ for IF; $t(30) = -2.9$, $p = .001$ for MD)] in patients compared to controls. The effects of CFs were also greater in controls in the ipsilateral FX [$t(30) = 3.1$, $p = .004$)] and PHC [$t(30) = 3.3$, $p = .003$)], suggesting more complex fiber structure in controls.

Correlation with clinical variables: Lower ND in the contralateral UNC was strongly associated with a longer disease duration ($r = .66$; $p = .003$), whereas there were no significant correlations between FA, MD, CF, or IF and any of the clinical variables in our patient cohort.

DISCUSSION

In this study, we better characterized underlying white matter changes in TLE using a new diffusion model, RSI, by separating intracellular changes in diffusion from extracellular changes as well as other possible factors like crossing fibers. In 21 patients with TLE compared to 11 age-matched controls, we found decreases in ND within the ipsilateral temporal lobe that appear to be a more sensitive measure of pathological change in TLE compared to FA. This decrease is in line with loss of axons and dendrites in the temporal lobe (Figure 3). These findings are encouraging as they match the broad pattern of decrease in ND/FA as reflected in our tract based analysis (Table 2) and match a growing wealth of literature suggesting that advanced diffusion imaging may provide a more sensitive measure of white matter pathology in epilepsy (Winston et al., 2015).

As seen in Figure 3, the expanse of significant change is primarily concentrated in regions proximal to the epileptogenic hippocampal region in the mesial temporal lobe. This reflects findings in studies which utilized DKI-derived measures (Glenn et al., 2016). Regions of exceptional note are white matter fibers extending to and from the temporal pole and those running parallel to the hippocampus. The relatively minor changes in IF and CF in tract analysis compared to changes in the restricted compartment suggests FA decreases are primarily driven by neurite loss, not other potentially confounding factors such as perpendicular fibers or inflammation. As FA is a measure of directionality of diffusion, FA decrease can form from perpendicular fibers or large

pockets of free diffusion, such as in inflammation. However, neither CF nor IF is of exceptional note for the most part in this VBA.

There is an interesting exception to the pattern of decreasing ND alongside decreasing FA within the PHC and FX ipsilateral to the seizure focus. Our analysis in this region has revealed a patch of white matter with complex microarchitecture suggesting highly crossed fibers in healthy subjects (Figure 3 and Table 3). In RTLE subjects in particular, these complex fiber arrangements appear to disappear as would be described by a lower CF value that may in turn inflate FA. As crossed fibers decrease the directionality of diffusion in DTI, we subsequently expect decreased FA in whole tract analysis involving tracts with regions of crossing white matter. CF and its confounding relationship to FA and epilepsy is further complicated by the possibility of selective or majority loss of tracts proximal to the epileptic zone. Epileptic tracts with formerly decreased FA due to perpendicularly crossed fibers could be theoretically confounded in these regions by increased directionality from increased FA and alleviated crossing effects. This situation likely plays out in the PHC, given the crossed nature of the performant path and adjacent pathway which run parallel along and from the entorhinal cortex into the hippocampus. Figure 4 depicts a representative voxel from both a TLE and control patient and exhibits the fundamental shape of the fibers in the region as modeled by DTI and RSI. RSI is more capable of capturing changes in complex architecture, as it is not limited to a simplified ellipsoid system. For much of the brain, it appears that lost neurites are the driving force behind lowered FA, but there are exceptions to be cautious of as exemplified by these confounding crossing fibers.

4.2 Tract Based Analysis

Tract-based analyses were also performed to further characterize our findings (Table 2 and Table 3). In LTLE, PHC and CING showed reductions in FA bilaterally, as did the left UNC, IFOF and FX. These results were mirrored with decreases in ND, as shown in the VBA maps. In patients with LTLE, a similar pattern was observed, with significant decreases in FA mirrored by significant changes in ND with a trending decrease of CF. There were instances of significant decreases in ND not mirrored by significant decreases in FA, such as in the right CING, ILF, IFOF and FX. as well as the left PHC and FORX. CF saw significant decreases in the right PHC and FX. Free water diffusion saw significant increases only in the right FX. These significant changes in CF and If are likely pathological as well, given the tract's exceptional proximity to the epileptogenic zone, though their relative contribution to explaining the deficiencies in FA is not as consistent as ND. These results in the tract based analysis complement our finding in the VBA by further specifying particular white matter tracts that are affected in TLE.

4.3 Advanced Registration

One of the major strengths of this project was the implementation of the ANTS toolbox in epilepsy. In a study of 14 nonlinear registration techniques, ANTS-SYN consistently outperformed other techniques, often to a significant degree (Klein et al., 2009). As of this thesis, there are no known implementations nor publications of ANTS-SYN based registrations in epilepsy research.

The use of T1 weighted structural scans to register subjects into central group-wise space for direct voxel to voxel comparisons builds on older intramodality registrations. The fallacy in using maps of FA to register other maps of FA is one of logical circularity. As any subject's FA map approaches a template FA, a registration algorithm will simply bias it to the next warp which lowers the variance, which causes inherent statistical bias (Tustison et al., 2014) This additional confounding factor calls into question the accuracy of many potentially false positives identified in previous studies showing vast regions of purported pathological change in epileptic patients.

4.4 Limitations and Future Directions

This study is the first to demonstrate the potential use of RSI in further elucidating the underlying white matter pathology in TLE. In the course of this study, both voxel wise and tract-based analysis of microstructure was undertaken with both results in agreeance. There were limitations to our study however, with our relatively small sample size in particular. There is a risk in potentially not having the power to detect subtle group differences in diffusion measures that might have been seen with a larger sample size. It is important to also note that we were able to capture robust associations with ND and large effect sizes even with our cohort size. This result could translate into few patients enrolled in clinical trials to demonstrate an effect when RSI- vs DTI-derived metrics are used. Another potential limitation of our study with the inclusion of patients both positive and negative for MTS. There is now considerable evidence that DTI-derived abnormalities are more pronounced in patients with radiological evidence of MTS (Concha et al., 2009). In our small sample, it is of note that patients with MTS

demonstrated a trend toward lower ND in the PHC relative to those without MTS ($p = .054$) and this likely contributed to the stronger patterns in FA and ND loss seen in the VBA maps in LTLE (the group with a greater number of patients with MTS) relative to RTLE. However, our group of MTS+ ($N = 8$) and MTS- ($N = 13$) were too small and unbalanced to analyze separately in this initial study. Future research with a larger patient sample will test the utility of RSI-derived measures in each patient cohort separately. While our multi-compartment diffusion model offers advantages over many existing models for better elucidating white matter changes within a clinically-feasible time frame, as with most diffusion techniques, histological validation of the RSI-model is primarily limited to preclinical data and will require further validation in patients with TLE and other epilepsy syndromes.

FIGURES AND TABLES

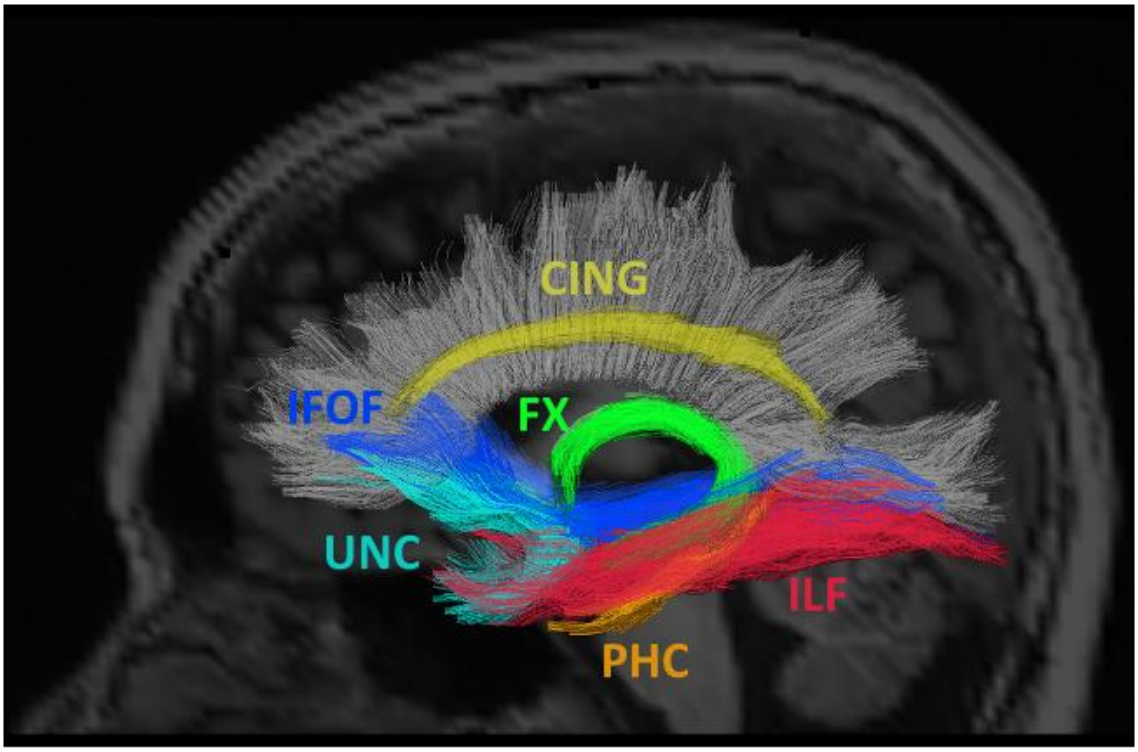

Figure 1: **Fiber Tracts** shown are inferior fronto-occipital fasciculus (IFOF), uncinated (UNC), fornix (FX), cingulum (CING), parahippocampal cingulum (PHC), and inferior longitudinal fasciculus (ILF).

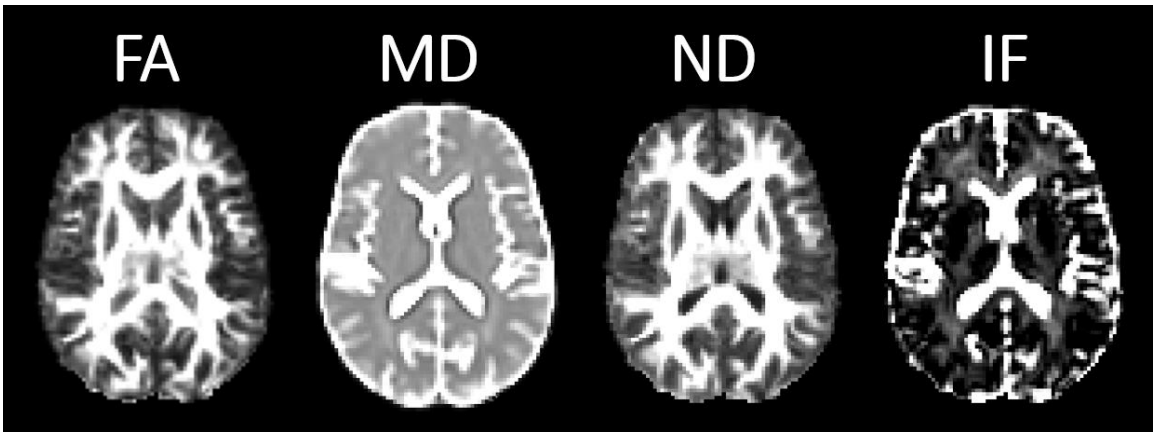

Figure 2: **Maps of Measures** Fractional Anisotrophy (FA), Mean Diffusivity (MD), Neurite Density (ND), and Isotropic Free (IF). Maps shown are native space maps derived from a healthy control.

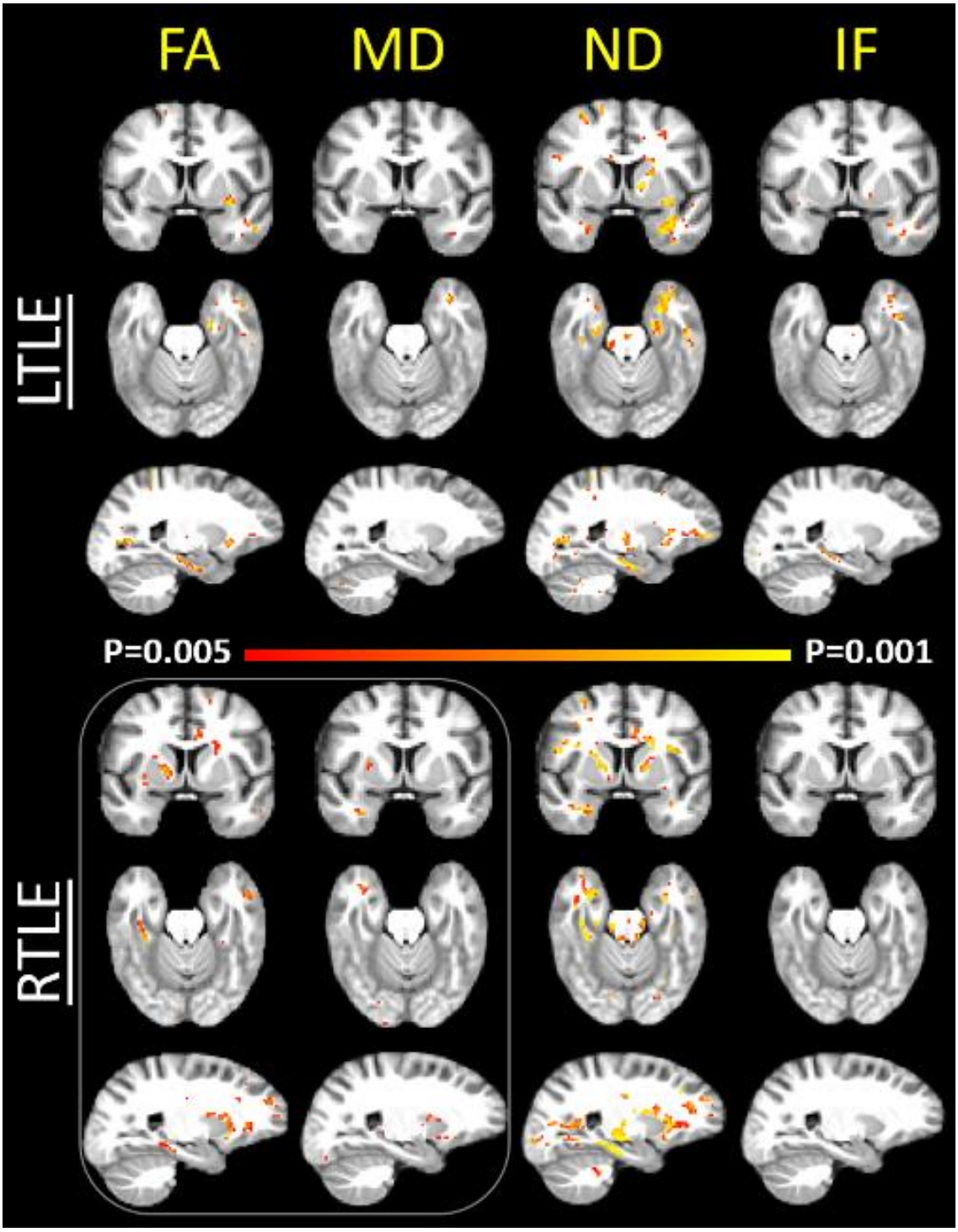

Figure 3: **Voxel Based Analysis of Measures:** fractional anisotropy(FA), mean diffusivity (MD), neurite density(ND), and free water diffusion(If) of white matter overlaid on groupwise generated T1-weighted whole brain atlases. P-Value maps were derived from comparisons between controls and patients further thresholded to the 0.005 to 0.001 range are shown with the exceptions of DTI derived RTLE FA and MD thresholded to 0.02 to 0.001. LTLE = left TLE; RTLE = right TLE

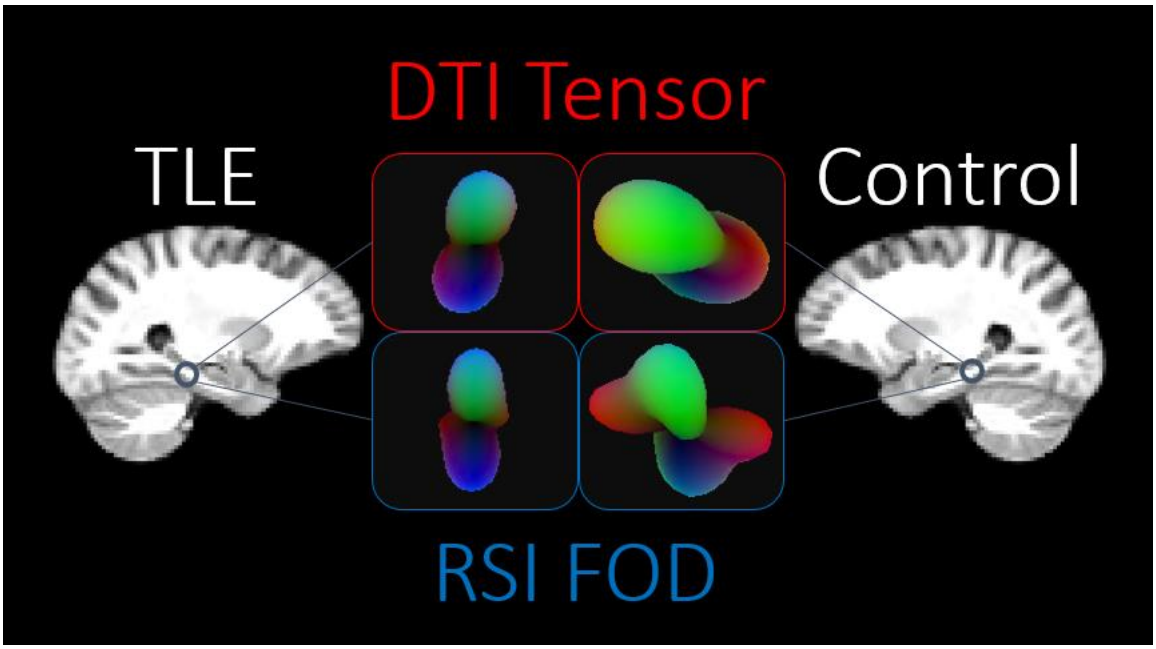

Figure 4: **Tensor to FOD** in TLE versus control in the parahippocampal cingulum. Significant declines in crossing fibers are exemplified by deteriorated TLE FOD. Less significant declines in FA from increasing anisotrophy are expected in TLE.

Table 1: **Patient Demographics**

Table 1	Control (n=11)	LTLE (n=10)	RTLE (n=11)
Age	37.79 (17.94)	43.50 (12.07)	38.09 (12.88)
Gender	8 M, 3 F	5 M, 5 F	5 M, 6 F
Education (years)	16.91 (2.77)	14.40 (1.65)	14.60 (2.37)
Age of Onset (years)	N/A	15.40 (19.24)	21.65 (16.72)
Duration (years)	N/A	28.20 (16.36)	17.65 (15.04)
MTS Status	N/A	5+, 5-	3+, 8-
Seizure Frequency (# per month)	N/A	10.70 (17.38)	6.12 (12.93)
Left Hippocampal Volume (mm^3)	4089.85 (396.85)	2843.76 (922.66)	3871.69 (669.41)
Right Hippocampal Volume (mm^3)	4115.62 (595.79)	3998.87 (434.87)	3699.19 (679.07)

Table 2: **FA and ND Analysis** of the ipsilateral and contralateral fiber tracts for Controls and Patients with TLE.

		Controls	TLEs			
		Mean	Mean	T-Score	p-value	Cohen's d
FX Ipsilateral*	FA	0.3030 (0.02137)	0.2353 (0.05535)	3.884	0.000524	1.6136
	ND	0.4354 (0.02860)	0.3011 (0.09440)	4.577	0.000077	1.9255
Contralateral	FA	0.3030 (0.02137)	0.2481 (0.05081)	3.412	0.001866	1.4085
	ND	0.4354 (0.02860)	0.3269 (0.08955)	3.89	0.000516	1.6322
CING Ipsilateral	FA	0.4719 (0.01929)	0.4101 (0.04546)	4.285	0.000173	1.7697
	ND	0.6698 (0.02674)	0.5799 (0.04676)	5.869	0.000002	2.3602
Contralateral	FA	0.4719 (0.01929)	0.4164 (0.04882)	3.601	0.001128	1.6649
	ND	0.6698 (0.02674)	0.5963 (0.05194)	4.379	0.000134	1.7792
PHC Ipsilateral*	FA	0.3434 (0.04255)	0.2163 (0.09259)	4.286	0.000183	1.7639
	ND	0.4828 (0.07161)	0.3012 (0.10740)	5.011	0.000025	1.9895
Contralateral	FA	0.3434 (0.04255)	0.2397 (0.10456)	3.136	0.003813	1.2991
	ND	0.4828 (0.07161)	0.3342 (0.11078)	4.016	0.000366	1.5931
UNC Ipsilateral	FA	0.4473 (0.03507)	0.3839 (0.05778)	3.302	0.002553	1.3265
	ND	0.6319 (0.03244)	0.5679 (0.07125)	2.809	0.004796	1.1561
Contralateral	FA	0.4473 (0.03507)	0.4180 (0.03775)	2.119	0.042812	0.8041
	ND	0.6319 (0.03244)	0.5940 (0.03041)	3.246	0.002948	1.2054
ILF Ipsilateral	FA	0.4733 (0.02371)	0.4441 (0.04467)	2.014	0.053091	0.8165
	ND	0.6773 (0.01661)	0.6379 (0.05623)	2.255	0.031604	0.9503
Contralateral	FA	0.4733 (0.02371)	0.4569 (0.04080)	1.224	0.230354	0.4914
	ND	0.6773 (0.01661)	0.6490 (0.04381)	2.055	0.048681	0.8542
IFOF Ipsilateral	FA	0.4885 (0.02485)	0.4733 (0.03149)	2.774	0.009435	0.5358
	ND	0.6854 (0.02462)	0.6394 (0.03284)	4.066	0.000318	1.5849
Contralateral	FA	0.4885 (0.02485)	0.4793 (0.03340)	0.806	0.426731	0.3125
	ND	0.6854 (0.02462)	0.6600 (0.03867)	1.968	0.058393	0.7835

Table 3: **Tract Based Analysis** T-Tests of white matter tracts regions of interest derived from AtlasTrack. *: P<0.01 **: P<0.005(significant) Tracts listed are the superior aspect of the cingulum(CING), the parahippocampal portion of the cingulum(PHC), the uncinated(UNC), the inferior longitudinal fasciculus(ILF), the inferior fronto-occipital fasciculus(IFOF) and a partial voluming resistant portion of the fornix(Fx).

	Left TLE											
	CING		**PHC**		**UNC**		**ILF**		**IFOF**		**FxCut**	
	L	**R**	**L**	**R**	**L**	**R**	**L**	**R**	**L**	**R**	**L**	**R**
FA	0.003**	0.000**	0.000**	0.000**	0.001**	0.091	0.140	0.183	0.002**	0.297	0.001**	0.016
ND	0.000**	0.007*	0.001**	0.001**	0.032	0.022	0.186	0.083	0.006*	0.129	0.000**	0.013
CF	0.097	0.621	0.065	0.083	0.147	0.785	0.510	0.240	0.962	0.656	0.010	0.208
If	0.153	0.625	0.006*	0.003**	0.114	0.522	0.016	0.098	0.049	0.133	0.003**	0.042
	Right TLE											
	CING		**PHC**		**UNC**		**ILF**		**IFOF**		**FxCut**	
	L	**R**	**L**	**R**	**L**	**R**	**L**	**R**	**L**	**R**	**L**	**R**
FA	0.001**	0.005*	0.035	0.005*	0.015	0.076	0.411	0.037	0.744	0.100	0.001**	0.003**
ND	0.000**	0.000**	0.004**	0.000**	0.009*	0.005*	0.032	0.002**	0.025	0.000**	0.000**	0.000**
CF	0.740	0.861	0.121	0.001**	0.763	0.623	0.268	0.538	0.135	0.564	0.001**	0.001**
If	0.138	0.801	0.022	0.003**	0.739	0.656	0.357	0.837	0.418	0.501	0.038	0.009*

REFERENCES

Abrahams, S., Pickering, A., Polkey, C.E. and Morris, R.G., 1997. Spatial memory deficits in patients with unilateral damage to the right hippocampal formation. Neuropsychologia, 35(1), pp.11-24.

Ahmadi, M.E., Hagler, D.J., McDonald, C.R., Tecoma, E.S., Iragui, V.J., Dale, A.M. and Halgren, E., 2009. Side matters: diffusion tensor imaging tractography in left and right temporal lobe epilepsy. American journal of neuroradiology, 30(9), pp.1740-1747.

Assaf, Y. and Pasternak, O., 2008. Diffusion tensor imaging (DTI)-based white matter mapping in brain research: a review. Journal of molecular neuroscience, 34(1), pp.51-61.

Avants, B.B., Tustison, N.J., Song, G., Cook, P.A., Klein, A. and Gee, J.C., 2011. A reproducible evaluation of ANTs similarity metric performance in brain image registration. Neuroimage, 54(3), pp.2033-2044.

Banerjee, P.N., Filippi, D. and Hauser, W.A., 2009. The descriptive epidemiology of epilepsy—a review. Epilepsy research, 85(1), pp.31-45.

Basser, P.J. and Jones, D.K., 2002. Diffusion-tensor MRI: theory, experimental design and data analysis–a technical review. NMR in Biomedicine, 15(7-8), pp.456-467.

Baxendale, S.A., Thompson, P.J. and Van Paesschen, W., 1998. A test of spatial memory and its clinical utility in the pre-surgical investigation of temporal lobe epilepsy patients. Neuropsychologia, 36(7), pp.591-602.

Beaulieu, C., 2002. The basis of anisotropic water diffusion in the nervous system‐a technical review. NMR in Biomedicine, 15(7‐8), pp.435-455.

Ben-Ari, Y., 1985. Limbic seizure and brain damage produced by kainic acid: mechanisms and relevance to human temporal lobe epilepsy. Neuroscience, 14(2), pp.375-403.

Brett, M., 1999. The MNI brain and the Talairach atlas.

Parent, A., 1996. Carpenter's human neuroanatomy. Williams & Wilkins.

Concha, L., Beaulieu, C., Collins, D.L. and Gross, D.W., 2009. White-matter diffusion abnormalities in temporal-lobe epilepsy with and without mesial temporal sclerosis. Journal of Neurology, Neurosurgery & Psychiatry, 80(3), pp.312-319.

Concha, L., Kim, H., Bernasconi, A., Bernhardt, B.C. and Bernasconi, N., 2012. Spatial patterns of water diffusion along white matter tracts in temporal lobe epilepsy. Neurology, 79(5), pp.455-462.

Diehl, B., Busch, R.M., Duncan, J.S., Piao, Z., Tkach, J. and Lüders, H.O., 2008. Abnormalities in diffusion tensor imaging of the uncinate fasciculus relate to reduced memory in temporal lobe epilepsy. Epilepsia, 49(8), pp.1409-1418.

Fischl, B., Salat, D.H., Busa, E., Albert, M., Dieterich, M., Haselgrove, C., Van Der Kouwe, A., Killiany, R., Kennedy, D., Klaveness, S. and Montillo, A., 2002. Whole brain segmentation: automated labeling of neuroanatomical structures in the human brain. Neuron, 33(3), pp.341-355.

Gastaut, H., Gastaut, J.L., Silva, G.E. and Sanchez, G.R., 1975. Relative frequency of different types of epilepsy: a study employing the classification of the International League Against Epilepsy. Epilepsia, 16(3), pp.457-461.

Glenn, G.R., Jensen, J.H., Helpern, J.A., Spampinato, M.V., Kuzniecky, R., Keller, S.S. and Bonilha, L., 2016. Epilepsy-related cytoarchitectonic abnormalities along white matter pathways. Journal of Neurology, Neurosurgery & Psychiatry, pp.jnnp-2015.

Gross, D.W., 2011. Diffusion tensor imaging in temporal lobe epilepsy. Epilepsia, 52(s4), pp.32-34.

Hagler, D.J., Ahmadi, M.E., Kuperman, J., Holland, D., McDonald, C.R., Halgren, E. and Dale, A.M., 2009. Automated white‐matter tractography using a probabilistic diffusion tensor atlas: Application to temporal lobe epilepsy. Human brain mapping, 30(5), pp.1535-1547.

Harvey, A.S., Berkovic, S.F., Wrennall, J.A. and Hopkins, I.J., 1997. Temporal lobe epilepsy in childhood: clinical, EEG, and neuroimaging findings and syndrome classification in a cohort with new-onset seizures. Neurology, 49(4), pp.960-968.

Hermann, B., Seidenberg, M., Lee, E.J., Chan, F. and Rutecki, P., 2007. Cognitive phenotypes in temporal lobe epilepsy. Journal of the International Neuropsychological Society, 13(01), pp.12-20.

Holland, D., Kuperman, J.M. and Dale, A.M., 2010. Efficient correction of inhomogeneous static magnetic field-induced distortion in Echo Planar Imaging. Neuroimage, 50(1), pp.175-183.

Jensen, J.H., Helpern, J.A., Ramani, A., Lu, H. and Kaczynski, K., 2005. Diffusional kurtosis imaging: The quantification of non‐gaussian water diffusion by means

of magnetic resonance imaging. Magnetic Resonance in Medicine, 53(6), pp.1432-1440.

Jezzard, P., Barnett, A.S. and Pierpaoli, C., 1998. Characterization of and correction for eddy current artifacts in echo planar diffusion imaging. Magnetic resonance in medicine, 39(5), pp.801-812.

Jones, D.K. and Cercignani, M., 2010. Twenty‐five pitfalls in the analysis of diffusion MRI data. NMR in Biomedicine, 23(7), pp.803-820.

Klein, A., Andersson, J., Ardekani, B.A., Ashburner, J., Avants, B., Chiang, M.C., Christensen, G.E., Collins, D.L., Gee, J., Hellier, P. and Song, J.H., 2009. Evaluation of 14 nonlinear deformation algorithms applied to human brain MRI registration. Neuroimage, 46(3), pp.786-802.

Klein, A., Ghosh, S.S., Avants, B., Yeo, B.T., Fischl, B., Ardekani, B., Gee, J.C., Mann, J.J. and Parsey, R.V., 2010. Evaluation of volume-based and surface-based brain image registration methods. NeuroImage, 51(1), pp.214-220.

Kothari, P.D., White, N.S., Farid, N., Chung, R., Kuperman, J.M., Girard, H.M., Shankaranarayanan, A., Kesari, S., McDonald, C.R. and Dale, A.M., 2013. Longitudinal restriction spectrum imaging is resistant to pseudoresponse in patients with high-grade gliomas treated with bevacizumab. American Journal of Neuroradiology, 34(9), pp.1752-1757.

Le Bihan, D., Breton, E., Lallemand, D., Grenier, P., Cabanis, E. and Laval-Jeantet, M., 1986. MR imaging of intravoxel incoherent motions: application to diffusion and perfusion in neurologic disorders. Radiology, 161(2), pp.401-407.

Lemkaddem, A., Daducci, A., Kunz, N., Lazeyras, F., Seeck, M., Thiran, J.P. and Vulliémoz, S., 2014. Connectivity and tissue microstructural alterations in right and left temporal lobe epilepsy revealed by diffusion spectrum imaging. NeuroImage: Clinical, 5, pp.349-358.

Liu, M., Concha, L., Lebel, C., Beaulieu, C. and Gross, D.W., 2012. Mesial temporal sclerosis is linked with more widespread white matter changes in temporal lobe epilepsy. NeuroImage: Clinical, 1(1), pp.99-105.

Meldrum, B., 1991. 9. Excitotoxicity and epileptic brain damage. Epilepsy research, 10(1), pp.55-61.

White, N.S., Leergaard, T.B., D'Arceuil, H., Bjaalie, J.G. and Dale, A.M., 2013. Probing tissue microstructure with restriction spectrum imaging: histological and theoretical validation. Human brain mapping, 34(2), pp.327-346.

Niendorf, T., Dijkhuizen, R.M., Norris, D.G., van Lookeren Campagne, M. and Nicolay, K., 1996. Biexponential diffusion attenuation in various states of brain tissue: Implications for diffusion‐weighted imaging. Magnetic Resonance in Medicine, 36(6), pp.847-857.

Nichols, T.E. and Holmes, A.P., 2002. Nonparametric permutation tests for functional neuroimaging: a primer with examples. Human brain mapping, 15(1), pp.1-25.

Otte, W.M., van Eijsden, P., Sander, J.W., Duncan, J.S., Dijkhuizen, R.M. and Braun, K.P., 2012. A meta‐analysis of white matter changes in temporal lobe epilepsy as studied with diffusion tensor imaging. Epilepsia, 53(4), pp.659-667.

Papadakis, N.G., Murrills, C.D., Hall, L.D., Huang, C.L.H. and Carpenter, T.A., 2000. Minimal gradient encoding for robust estimation of diffusion anisotropy☆. Magnetic Resonance Imaging, 18(6), pp.671-679.

Pierpaoli, C. and Basser, P.J., 1996. Toward a quantitative assessment of diffusion anisotropy. Magnetic resonance in Medicine, 36(6), pp.893-906.

Wakana, S., Van Zijl, P.C. and Nagae-Poetscher, L.M., 2005. MRI atlas of human white matter (Vol. 16). Amsterdam:: Elsevier.

Smith, S.M., 2002. Fast robust automated brain extraction. Human brain mapping, 17(3), pp.143-155.

Sabsevitz, D.S., Swanson, S.J., Hammeke, T.A., Spanaki, M.V., Possing, E.T., Morris, G., Mueller, W.M. and Binder, J.R., 2003. Use of preoperative functional neuroimaging to predict language deficits from epilepsy surgery. Neurology, 60(11), pp.1788-1792.

Smith, S.M. and Nichols, T.E., 2009. Threshold-free cluster enhancement: addressing problems of smoothing, threshold dependence and localisation in cluster inference. Neuroimage, 44(1), pp.83-98.

Smith, S.M., Jenkinson, M., Johansen-Berg, H., Rueckert, D., Nichols, T.E., Mackay, C.E., Watkins, K.E., Ciccarelli, O., Cader, M.Z., Matthews, P.M. and Behrens, T.E., 2006. Tract-based spatial statistics: voxelwise analysis of multi-subject diffusion data. Neuroimage, 31(4), pp.1487-1505.

Téllez-Zenteno, J.F., Dhar, R. and Wiebe, S., 2005. Long-term seizure outcomes following epilepsy surgery: a systematic review and meta-analysis. Brain, 128(5), pp.1188-1198.

Tellez‐Zenteno, J.F., Patten, S.B., Jetté, N., Williams, J. and Wiebe, S., 2007. Psychiatric comorbidity in epilepsy: a population‐based analysis. Epilepsia, 48(12), pp.2336-2344.

Tustison, N.J., Avants, B.B., Cook, P.A., Kim, J., Whyte, J., Gee, J.C. and Stone, J.R., 2014. Logical circularity in voxel‐based analysis: Normalization strategy may induce statistical bias. Human brain mapping, 35(3), pp.745-759.

Vincent, P. and Mulle, C., 2009. Kainate receptors in epilepsy and excitotoxicity. Neuroscience, 158(1), pp.309-323.

Vulliemoz, S., Vollmar, C., Koepp, M.J., Yogarajah, M., O'Muircheartaigh, J., Carmichael, D.W., Stretton, J., Richardson, M.P., Symms, M.R. and Duncan, J.S., 2011. Connectivity of the supplementary motor area in juvenile myoclonic epilepsy and frontal lobe epilepsy. Epilepsia, 52(3), pp.507-514.

Wehner, T., Lapresto, E., Tkach, J., Liu, P., Bingaman, W., Prayson, R.A., Ruggieri, P. and Diehl, B., 2007. The value of interictal diffusion-weighted imaging in lateralizing temporal lobe epilepsy. Neurology, 68(2), pp.122-127.

Wieser, H.G., 2004. ILAE Commission Report. Mesial temporal lobe epilepsy with hippocampal sclerosis. Epilepsia, 45(6), pp.695-714.

Winkler, A.M., Ridgway, G.R., Webster, M.A., Smith, S.M. and Nichols, T.E., 2014. Permutation inference for the general linear model. Neuroimage, 92, pp.381-397.

Winston, G.P., Stretton, J., Sidhu, M.K., Symms, M.R., Thompson, P.J. and Duncan, J.S., 2013. Structural correlates of impaired working memory in hippocampal sclerosis. Epilepsia, 54(7), pp.1143-1153.

Winston, G.P., 2015. The potential role of novel diffusion imaging techniques in the understanding and treatment of epilepsy. Quantitative imaging in medicine and surgery, 5(2), p.279.

Wong, M. and Guo, D., 2013. Dendritic spine pathology in epilepsy: cause or consequence?. Neuroscience, 251, pp.141-150.

Zhang, Y., Brady, M. and Smith, S., 2001. Segmentation of brain MR images through a hidden Markov random field model and the expectation-maximization algorithm. Medical Imaging, IEEE Transactions on, 20(1), pp.45-57.